RESEARCH ARTICLE

Facile Synthesis and Investigation of Flower like p-NiO/n-ZnO as Efficient Photocatalyst for Degradation of Erythromycin under Sunlight

Sajad Khamani [1], Mohammad Hossein Ghorbani [2,], Leila Torkian [3], Reza Fazaeli[4], Zahra Khodadadi [5]*

[1] *Department of applied chemistry, South Tehran Branch, Islamic Azad University, Tehran, Iran*

[2] *Department of Chemical engineering, Faculty of engineering, South Tehran Branch, Islamic Azad University, Tehran, Iran*

[3] *Department of applied chemistry, South Tehran Branch, Islamic Azad University, Tehran, Iran*

[4] *Department of Chemical engineering, Faculty of engineering, South Tehran Branch, Islamic Azad University, Tehran, Iran*

[5] *Department of applied chemistry, South Tehran Branch, Islamic Azad University, Tehran, Iran*

ARTICLE INFO

Article History:
Received 2021-12-19
Accepted 2022-01-26
Published 2022-12-22

Keywords:
NiO/ZnO,
Antibiotic,
Erythromycin,
Degradation,
Sunlight.

ABSTRACT

Conventional wastewater treatment is not able to effectively removal drugs such as antibiotics, so it is important to remove the remaining antibiotics from the environment. In this research, Zinc oxide (ZnO), nickel oxide (NiO) and p-NiO/n-ZnO heterostructure were synthesized. Then, prepared samples were characterized by several techniques. The photocatalytic degradation of erythromycin from aqueous solutions was studied by photocatalysts synthesized under sunlight. Design of Experimental (DOE) was used to evaluate the effective parameters in the degradation process of erythromycin. The effects of pH, time (min), photocatalytic mass (g) and erythromycin concentration (mg/L) were studied. Using Design Expert 7 software, the highest degradation efficiency of erythromycin was found 99.54%, under optimum conditions at pH 3.07, time 101.14 (min), photocatalyst mass 0.13 (g) and erythromycin concentration 41.04 (mg/L). Isotherm studies demonstrate that the experimental data are in good agreement with the 4-parameter Fritz-Schlander isotherm with the highest correlation coefficient.

How to cite this article
Khamani S., Ghorbani M. H., Torkian L., Fazaeli R., Khodadadi Z., Facile Synthesis and Investigation of Flower like p-NiO/n-ZnO as Efficient Photocatalyst for Degradation of Erythromycin under Sunlight. J. Nanoanalysis., 2022; 9(4): 251-264.
DOI: 10.22034/jna.2022.1946948.1286

INTRODUCTION

In recent years, due to the increasing use of antibiotics, and their continuous entry into the environment, extensive research has been conducted on the impact of antibiotics on human health, pollution of water resources and the environment. Drugs and pharmaceutical compounds are produced and consumed continuously with an upward trend in large volumes while the number of consumers and the variety of drugs are added every year. The presence of drug compounds in the environment and their continuous increase has raised a global concern [1]. Some over-the-counter drugs accumulate in the environment due to their long half-life. In addition to medicine, the use of antibiotics has increased significantly in agriculture, livestock, poultry, fish and aquaculture, and in the production of agricultural products, so the resistance to antibiotics, agriculture and the environment. Affects and ultimately the use of these agricultural products with antibiotics by humans and the entry of these substances into the body and excreted without changing some of these antibiotics from the human body causes it to enter the environment [2]. Antibiotics enter

* Corresponding Author Email: *mh_ghorbani@azad.ac.ir*

surface and groundwater resources and ultimately the environment through wastewater from various industries such as the pharmaceutical industry, hospital wastewater and agricultural runoff, as well as domestic wastewater. These substances have received special attention due to their ability to induce antibiotic resistance in pathogenic bacteria. Antibiotic resistance in microorganisms causes serious public health problems such as: difficulty in treating diseases, increased use of antibiotics and the need to produce more antibiotics and ultimately upset the balance of microbial populations in the ecosystem [3-7]. Erythromycin is a macrolide antibiotic that inhibits bacterial protein synthesis by binding reversibly to the S 50 ribosome and has a bacteriostatic effect, but is also bactericidal in high concentrations. Following oral administration, it is absorbed from the gastrointestinal tract and rapidly spreads to all tissues, cavities and body fluids. The drug is excreted mainly in the bile and to some extent in the urine. Erythromycin is effective against aerobic and anaerobic gram-positive bacteria such as Mycoplasma and Clostridia, Chlamydia, Bacillus anthracis, Corynebacterium, Listeria, Mycobacterium and Rickettsiae, while it is effective against protozoa, fungi and whole gram-negative bacteria. , Pseudomonas and E-coli have little effect. Erythromycin is given orally to treat local and general infections such as bronchopneumonia, bacterial enteritis, urinary tract infections, metritis and arthritis in livestock, upper respiratory tract infections, crease, sinusitis, C.R.D complex and enteritis in poultry [8-10]. Various methods are used to removing organic material from industrial effluents, including biological methods, coagulation/flocculation, electrocoagulation, adsorption on carbon, and so on. In these methods, due to the production of secondary pollutants, further treatment is required. In this case, the use of other complementary methods such as advanced oxidation processes (AOPs) is recommended [11-14]. This process has a great potential to eliminate all types of pollution and its applications include groundwater treatment, sludge degradation of industrial effluents and removal of volatile organic pollutants [15-20]. ZnO is a n-type semiconductor with a band gap has ranged from 3.10 eV to 3.37 eV. ZnO is one of the richest nanostructures in terms of morphological and application diversity. This diversity in morphology gives rise to unique features and applications in it. This material has spherical, sheet, tube, rod, flower-like and star morphologies [21, 22]. ZnO is a metal oxide widely used in various industries due to its biocompatibility and safety including sunscreens, electrodes and biosensors, photocatalysis, and solar cells. ZnO also has moisturizing, antibiotic and deodorant properties. ZnO is widely used due to its semiconductor, wide band gap, high thermal resistance, pyroelectric and piezoelectric properties in addition to medical applications in other industries including water and wastewater treatment, optics, electronics, rubber, plastic, ceramics, glass, wood, cement, paint and glue [23]. NiO has also attracted much scientific research due to its magnetic and electronic properties. NiO semiconductor is a p-type which energy band gap has been experimentally obtained at 2.7-4 eV. NiO network defects play a key role in the amount of energy gap. Also, NiO is a promising material for applications in fuel cell, photocatalysts, electrochemical capacitors, etc. [24-28]. Inspired by the above facts, it is very important to design p-NiO/n-ZnO heterojunction for studying their photocatalytic properties [29, 30]. In recent years, the use of statistical methods to design experiments in various fields of science and engineering has been considered by researchers. Classical methods for achieving the optimal value in experiments have various disadvantages, the most important of which is the large number of experiments. Using a variety of test design methods such as Taguchi methods and RSM can eliminate these disadvantages [31, 32]. The application of these statistical methods has higher accuracy, less number of tests, less time and minimal cost of tests compared to conventional classical methods. Li et al. investigated rational construction of a direct Z-scheme g-C3N4/CdS photocatalyst with enhanced visible light photocatalytic activity and degradation of erythromycin and tetracycline [33]. Fernández et al. were insight into antibiotics removal: Exploring the photocatalytic performance of a Fe3O4/ZnO nanocomposite in a novel magnetic sequential batch reactor [34]. In this study, flower like p-NiO/n-ZnO (5%) and p-NiO/n-ZnO heterostructure were synthesized. The degradation of erythromycin was investigated by the synthesized photocatalysts. Then CCD-based RSM was used to investigate the parameters affecting the photocatalytic degradation of erythromycin and optimizing operating conditions. Also, 2, 3 and 4 parameter adsorption isotherms were studied.

EXPERIMENTAL

Materials and Methods

Zinc Acetate Dihydrate (Zn (CH3COO)2. 2H2O 98%), Ammonia (NH3 25%), Nickel Chloride (NiCl2), Sodium oxalate (Na2C2O4), Ethylene Glycol were purchased from Sigma-Aldrich Company. Erythromycin (C37H67NO13 20%) was prepared by Jahan Daroo Alborz Company. The chemical structure of erythromycin is demonstrated in Fig. 1.

Synthesis of ZnO flower like particles

3.2 g of Zn (CH3COO)2. 2H2O was poured into 9 mL of NH3 and 50 mL distilled water. The resulting mixture was placed on a magnetic heater at 80 ° C for 6 h. The particles were then washed and put in an oven at 60 ° C for 2 h [35].

Synthesis of NiO particles

0.15 g of NiCl2, 0.03 g of Na2C2O4 were poured into 40 mL of EG and placed on a stirrer for 2 h. The prepared solution was poured into a hydrothermal autoclave and placed at 160 °C for 18 h. The obtained precipitate was washed with distilled water and then placed in an oven at 100 ° C for 1 h and then in a furnace at 500 ° C for 1 h [36].

p-NiO/n-ZnO flower like particles

1 g of ZnO with different amounts of 1, 2, 5 and 7 (wt(%)) NiO was poured into 200 mL of ethanol. The mixture stirred for 12 h and put in an oven at 120 ° C for 1 h.

Photocatalytic degradation

Experiments at pH=7, concentration of erythromycin =25 mg/L, NiO loading percentage (1, 2, 5 and 7 (wt(%)), mass of NiO, ZnO and flower like p-NiO/n-ZnO= 0.1 g and time 120 min under sunlight irradiation carried out. The samples were centrifuged at 4,000 rpm for 30 min. At that time, its absorption was measured by UV-visible spectroscopy at 298 nm.

$$\text{Efficiency} = \frac{(A_0 - A_t)}{A_0} * 100 \quad (1)$$

Where A0 is the initial absorption of erythromycin and At is its final absorption on the degradation.

DOE

In this study, RSM was used to model the degradation process. RSM is a powerful tool for statistical modeling that performs the least number of experimental experiments according to the experimental design. RSM itself has different types and this statistical method can be used in different ways. Two common methods of central composite design (CCD) and Box–Behnken design (BBD) are RSM. One of the most common methods used to optimize various factors is the use of a CCD. This design is an alternative and suitable method for factorial design. The advantage of using a CCD over a factorial design is the possibility of extracting more information from the analysis of this design and the smaller number of experiments

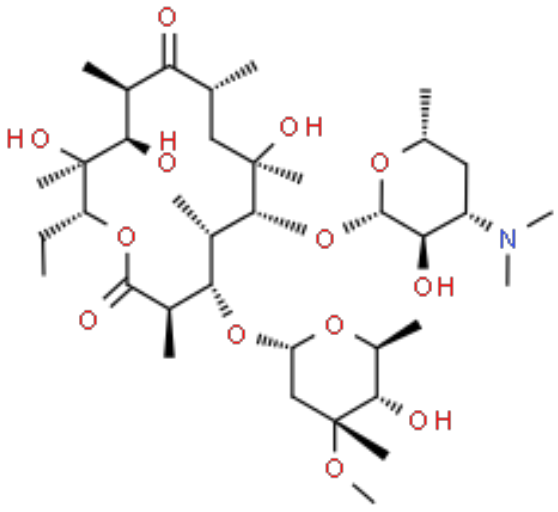

Fig. 1. Configuration of erythromycin molecule.

Table 1. Independent variables and their levels in the experimental.

Independent variables	Coded symbols	Levels
pH	X_1	2, 3.75, 5.5, 7.25, 9
Time (min)	X_2	10, 37.5, 65, 92.5, 120
Mass of catalyst (g)	X_3	0.02, 0.07, 0.11, 0.16, 0.2
Concentration of erythromycin (mg/L)	X_4	10, 27.5, 45, 62.5, 80

Table 2. Lists of adsorption isotherms models.

Isotherm	Nonlinear form	Isotherm	Nonlinear form	Isotherm	Nonlinear form
2 Parameters		3 Parameters		4 Parameters	
Langmuir	$q_e = \frac{q_m \times b \times C_e}{1 + b \times C_e}$	Redlich-Peterson	$q_e = \frac{K_R \times C_e}{1 + a_R \times C_e^g}$	Fritz-Schlunder	$q_e = \frac{C \times C_e^{\alpha_{FS}}}{1 + D \times C_e^{\beta_{FS}}}$
Freundlich	$q_e = K_f \times C_e^{1/n}$	Khan	$q_e = \frac{q_s \times b_K \times C_e}{(1 + b_K \times C_e)^{a_K}}$		
Tempkin	$q_e = B_T \times ln(A_T \times C_e)$	Radke-Prausnitz	$q_e = \frac{a_{RP} \times r_{RP} \times C_e}{1 + r_{RP} \times C_e^{B_{RP}}}$		

and iterations required to perform the experiment, which makes the implementation of this design easier.

The main regression equation to predict the effect of factors on the response is defined as follows:

$$Y = \beta_0 + \sum_{j=1}^{k} \beta_j X_j + \sum_{j=1}^{k} \beta_j X_j^2 + \sum_{i} \sum_{<j=2}^{k} \beta_j X_i X_j + e_i \quad (2)$$

50 mL of erythromycin with different concentrations of 10-80 (mg/L) were prepared at pH 2-9 and with different mass of catalyst of 0.02-0.2 (g) flower like p-NiO/n-ZnO (5%) was exposed to sunlight for 10-120 (min) Table 1. Also, under optimal conditions, the experiment was performed in the dark without sunlight.

Isotherm studies

50 mL of erythromycin was prepared with different concentrations of 20-120 (mg/L) at pH=3. Then 0.13 (g) flower like p-NiO/n-ZnO (5%) was poured into it and placed under sunlight for 100 (min). The photocatalytic degradation of erythromycin by p-NiO/n-ZnO (5%) photocatalyst was investigated under solar irradiation with isothermal equations of 2, 3 and 4 parameters and was minimized by 3 types of errors. The calculated isotherms and errors are shown in Tables 2 and 3, respectively [37].

Using Equation (3), the values of qe were calculated and plotted against Ce.

$$q_e = \frac{(C_0 - C_e)V}{W} \quad (3)$$

Here, qe is the mass of pollutant adsorbed per unit mass of catalyst, C0 and Ce are the initial and final concentrations of erythromycin, respectively. V is the volume of erythromycin solution (L) and W is the mass of the catalyst (g).

RESULTS AND DISCUSSION

The ZnO Flower like, NiO and p-NiO/n-ZnO flower like catalyst were synthesized and analyzed by XRD technique. The XRD analysis results of the ZnO flower-like catalyst are shown in Fig. 2. The XRD pattern of ZnO flower like at 2θ of 31.79, 34.42, 36.25, 47.51, 56.60, 62.86, 67.96 and 69o corresponds to the crystal faces (100), (002), (101), (110), (103), (112), and (201), respectively and has a cube of sphalerite phase (JCPDS-00-036-1451). The XRD pattern of NiO at 2θ of 37.24, 43.27, and 62.87o corresponds to the Miller indices (111), (200), and (220), respectively and has a cubic phase (JCPDS-00-047-1049) [36]. In p-NiO/n-ZnO flower like the peaks at diffraction angles 31.79, 34.42, 36.25, 47.51, 56.60, 62.86, 67.96 and 69o and 37.24, 43.27, and 62.87o are related to ZnO flower like and NiO, respectively [36]. According to

Table 3. Explanation of different error functions.

Error function	Abbreviation	Definition/expression
Hybrid fractional error function	HYBRID	$\frac{1}{n}=\sum_{i=1}^{n}\left[\frac{(q_{exp}-q_{cal}{}^{2})}{q_{exp}}\right]_i$
Marquardt's percent standard deviation	MPSD	$\frac{1}{n}=\sum_{i=1}^{n}\left[\frac{(q_{e,exp}-q_{e,cal})}{q_{e,exp}}\right]_i^2$
Average relative error	ARE	$\frac{1}{n}=\sum_{i=1}^{n}\left\|\frac{q_{exp}-q_{cal}}{q_{exp}}\right\|_i$

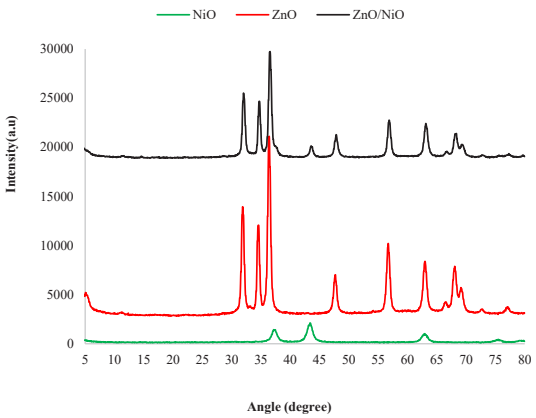

Fig. 2. XRD pattern of NiO, ZnO and NiO/ZnO.

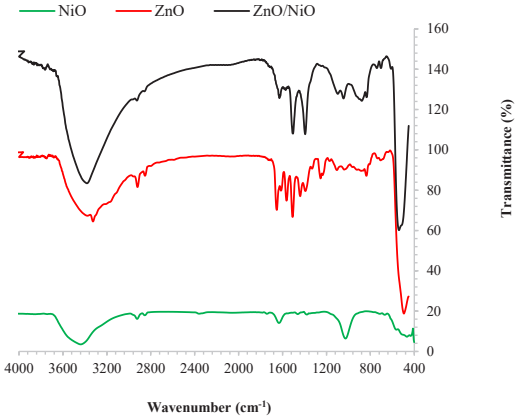

Fig. 3. FT-IR spectrum of NiO, ZnO and NiO/ZnO.

Equation (4), the average particle size was estimated according to Debye–Scherrer:

$$B=\frac{K\lambda}{L\cos\theta} \quad (4)$$

The average particle size calculated from the Debye–Scherrer for ZnO, NiO and flower like p-NiO/n-ZnO were about 76 nm 31 and 83 nm, respectively.

The vibrational properties of ZnO, NiO, and flower like p-NiO/n-ZnO catalysts were investigated by FT-IR spectroscopy. In the FT-IR spectrum of ZnO the band at 494.62 cm-1 characteristic to Zn-O bond. The peak at 1508.61 cm-1 is assigned to, O-H-O bond. The peaks at 1652.23 and 3326.01 cm-1 characteristic H-O-H and O-H stretching bond, respectively. In the FT-IR spectrum of NiO, peaks at 432.37 and 471.03 cm-1 are assigned to the Ni-O bond. The bonds at 1639.94 and 3448.51 cm-1, are characteristic to O-H-O and O-H, respectively [36]. In FT-IR spectrum of p-NiO/n-ZnO the peak appeared at 511.98 cm-1 is related to Ni-O, and that of 539.65 cm-1 is attributed to Zn-O bond, also the peaks at 1628.78 and 3380.78 cm-1 are related to H-O-H and O-H stretching, respectively (Fig. 3).

ZnO, NiO, and p-NiO/n-ZnO flower like were investigated by SEM, (Fig. 4). SEM results demonstrate that ZnO and NiO particles have a flower and spherical morphology, respectively, and are in nanoscale. Moreover, based on the results, NiO particles on the ZnO flower are well loaded.

The Xmap technique examines point-by-point a specific area of the sample. In this technique, EDS analysis is performed from a large number of points

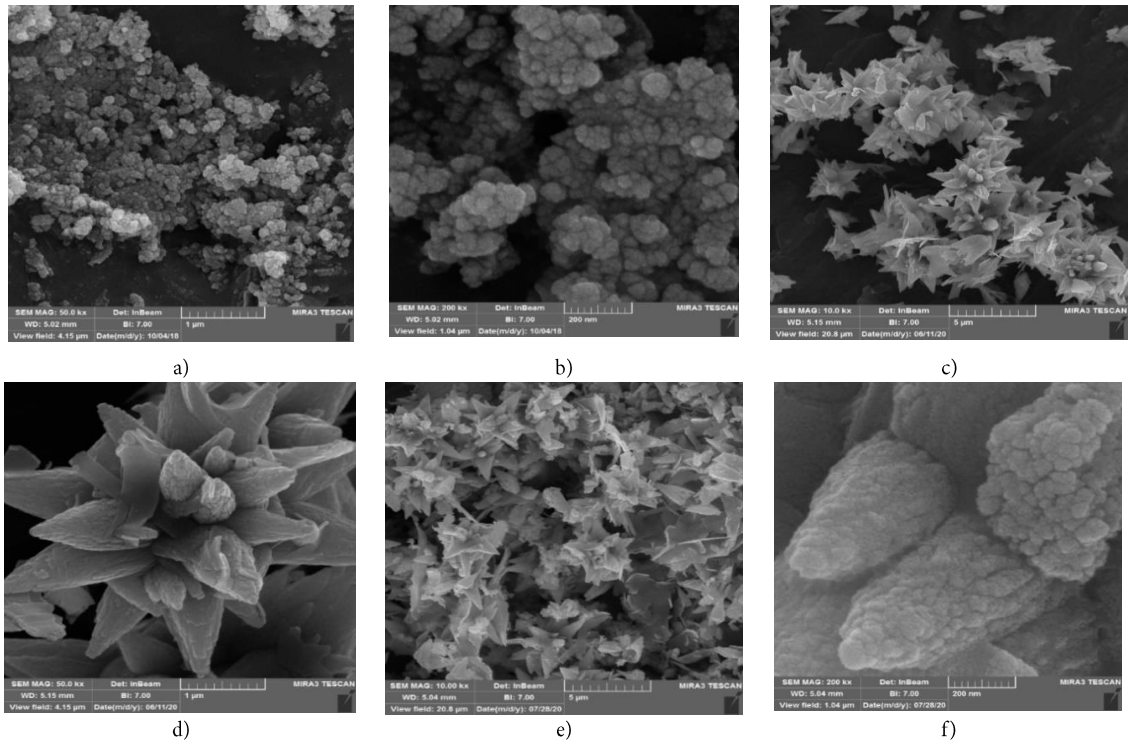

a) b) c)

d) e) f)

Fig. 4. SEM images of a,b) NiO, c,d) ZnO e,f) NiO/ZnO.

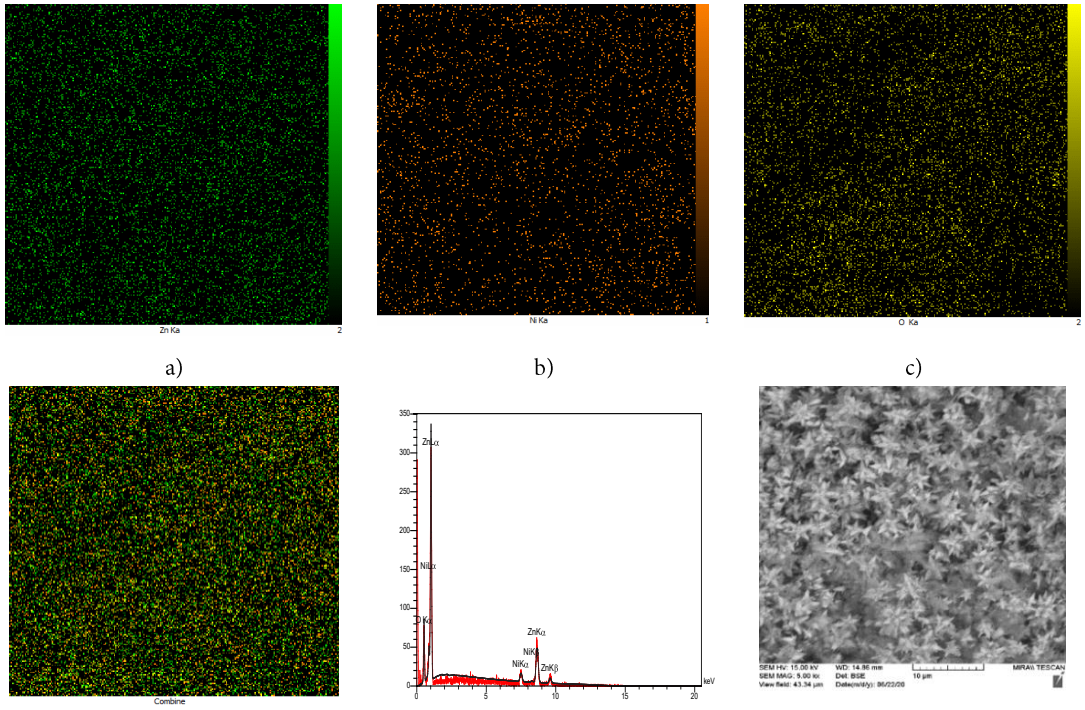

a) b) c)

(d) (e) f)

Fig. 5. Map images of a) Zn, b) Ni, c) O, d) combine, e) EDS pattern of NiO/ZnO and f) SEM of NiO/ZnO.

Table 4. Results of BET/BJH analysis for various catalysts.

Catalyst	as, BET ($m^2 g^{-1}$)	Total pore volume ($cm^3 g^{-1}$)	Mean pore diameter (nm)
ZnO	2.67	0.024	37.03
NiO	64.88	0.257	15.84
NiO/ZnO	5.33	0.029	35.48

in a specified area and the results of this analysis are displayed as a series of colored dots. Each color represents an element. Where the amount of this element is greater, the number of dots with that particular color is greater. In p-NiO/n-ZnO map images, the green, red and yellow dots indicate the presence of Zn, Ni, and O, respectively (Fig. 5). Based on the EDS results, the presence of O (21.47%), Zn(74.02%), and Ni (4.51%) elements in p-NiO/n-ZnO confirms that, with the exception of these elements, no other element was found in the sample indicating the formation of a high purity p-NiO/n-ZnO hybrid (Fig. 5).

BET specific surface measurement analysis is a physical analysis method for examining specific surface area and material porosity. This method, which is based on calculating the adsorption and desorption of gases such as nitrogen, is a fast and relatively inexpensive method that can be analyzed by statistically estimating the surface size, average particle size, porosity, porosity shape and porosity size materials obtained. The results for NiO, ZnO, and p-NiO/n-ZnO are demonstrated in Fig. 6 and Table 4. According the results, synthetic catalysts are of isotherm type IV. By loading NiO on ZnO, the surface area, pore volume and mean pore are increased.

There are different methods for estimating the optical band gap energy of semiconductor nanostructures, one of the most famous of which is the use of the Tauc equation.

$$(\alpha h\nu)\ 1/n = A\ (h\nu - Eg) \quad (5)$$

In this study, DRS and Tauc diagram were used to investigate the transfers and determine the band gap energy of the prepared photocatalysts. According to the results, the band gaps of ZnO, NiO and flower like p-NiO/n-ZnO were obtained as eV 3.3, 1.8, and 2.4, respectively (Fig. 7).

Effect of loaded NiO(%)

The weight percentage of metal oxides has a great effect on the performance of the photocatalyst. In this study, to optimize the weight percentage of NiO loaded on ZnO mud, NiO with weight percentages of 1, 2, 5 and 7 were prepared and used for photocatalytic degradation. The results demonstrate that by increasing the weight percentage of NiO from 1 to 5(wt %), the degradation efficiency increased from 78.45 to 98.56%. However, with increasing NiO (wt %) from 5 to 7, the photocatalytic degradation efficiency decreased from 98.56 to 63.85% (Fig. 8). By increasing the weight percentage of NiO from 5 to 7, the cavities of the ZnO photocatalyst are filled and the light penetration into the surface of the catalyst is decreased and, as a result, the efficiency is decreased.

Statistical analysis

The results of photocatalytic degradation of erythromycin by CCD method are demonstrated in Table 5.

One of the important issues in statistical analysis of data is the normal distribution of data, the results of this study are shown in Fig. 9.

Statistical evaluation was performed by performing F-test and ANOVA analysis of variance of the quadratic model of response surface and the result is given in Table 6. ANOVA data confirm the accuracy of this quadratic model. Parameter F is a measure of the deviation of the data from the mean value. In general, for a model that successfully predicts test results, F-value is usually very high and P-values of less than 0.05 mean that the model is desirable. F-value for this model is 42.77, which indicates that the model is completely significant. On the other hand, the value of parameter R-Squared is 0.9721 which is in accordance with Adj R-Squared 0.9460 values, and indicates the accuracy of the model.

Fig. 10 shows the disturbance diagram for photocatalytic degradation of erythromycin. Based on the obtained results, it can be concluded that the pH parameter (parameter A) has the greatest effect on the photocatalytic degradation of erythromycin.

Effect of pH and time on erythromycin degradation efficiency

The initial pH of the solution is one of the

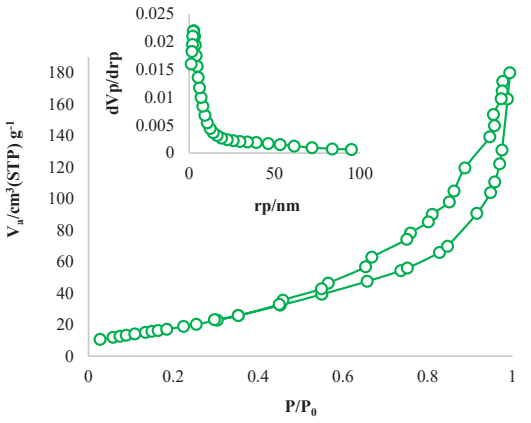

(a)

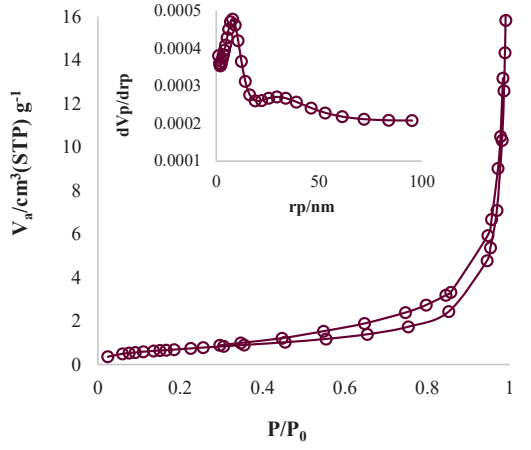

(b)

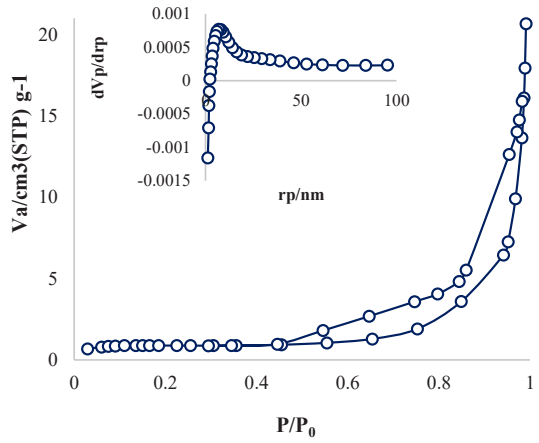

(c)

Fig. 6. N_2 adsorption-desorption isotherms of the a) NiO b) ZnO and c) NiO/ZnO.

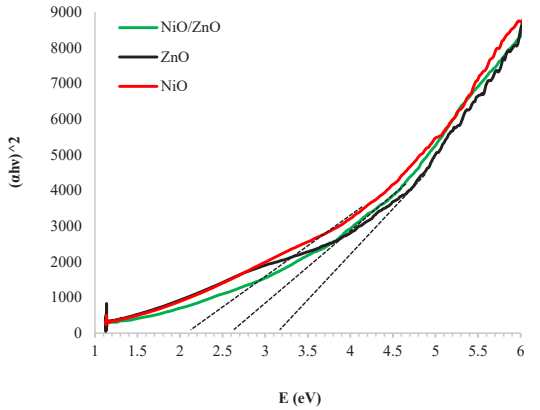

Fig. 7. Band gap energies of NiO, ZnO, NiO/ZnO.

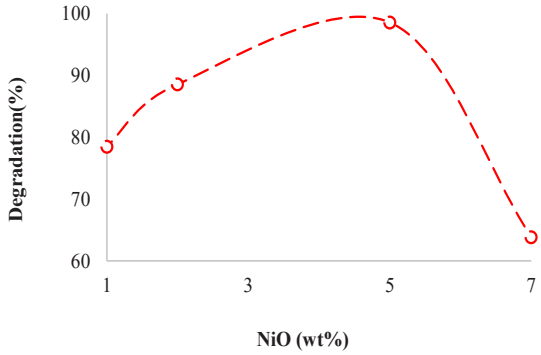

Fig. 8. Effect of weight percentage of loaded NiO.

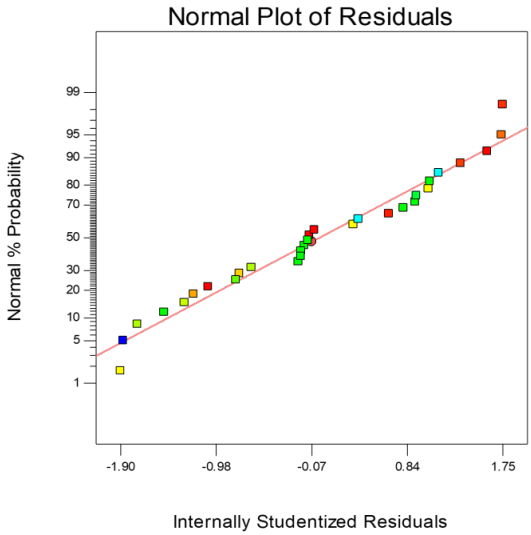

Fig. 9. Normal probability plot of the studentized residual for degradation of erythromycin.

Table 5. The CCD for the 4 independent variables.

STD	Run	pH	Time (min)	Mass of catalyst (g)	Concentration (mg/L)	Degradation (%)
7	1	3.75	92.50	0.16	27.50	99.43
5	2	3.75	37.50	0.16	27.50	77.35
11	3	3.75	92.50	0.07	62.50	97.54
24	4	5.50	65.00	0.11	80.00	66.87
30	5	5.50	65.00	0.11	45.00	62.53
9	6	3.75	37.50	0.07	62.50	94.36
17	7	2.00	65.00	0.11	45.00	91.89
6	8	7.25	37.50	0.16	27.50	80.65
10	9	7.25	37.50	0.07	62.50	49.53
16	10	7.25	92.50	0.16	62.50	60.54
19	11	5.50	10.00	0.11	45.00	73.42
29	12	5.50	65.00	0.11	45.00	62.54
12	13	7.25	92.50	0.07	62.50	50.34
14	14	7.25	37.50	0.16	62.50	66.34
1	15	3.75	37.50	0.07	27.50	76.54
28	16	5.50	65.00	0.11	45.00	62.45
18	17	9.00	65.00	0.11	45.00	32.54
25	18	5.50	65.00	0.11	45.00	62.64
27	19	5.50	65.00	0.11	45.00	65.87
13	20	3.75	37.50	0.16	62.50	87.98
26	21	5.50	65.00	0.11	45.00	62.76
23	22	5.50	65.00	0.11	10.00	93.87
4	23	7.25	92.50	0.07	27.50	79.65
21	24	5.50	65.00	0.02	45.00	76.54
2	25	7.25	37.50	0.07	27.50	64.23
15	26	3.75	92.50	0.16	62.50	89.65
22	27	5.50	65.00	0.20	45.00	97.65
3	28	3.75	92.50	0.07	27.50	99.54
20	29	5.50	120.00	0.11	45.00	95.11
8	30	7.25	92.50	0.16	27.50	85.95

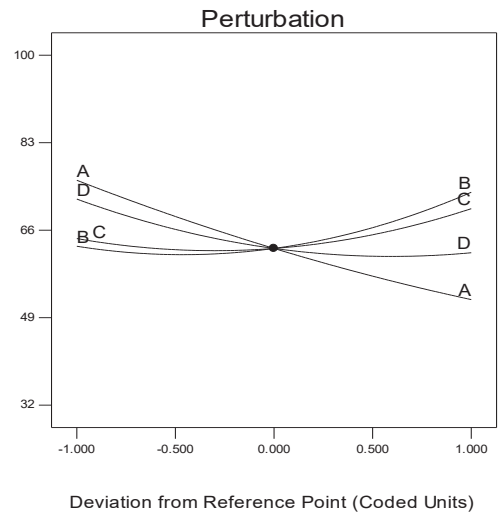

Fig. 10. Perturbation plot for degradation of erythromycin.

Table 6. ANOVA for analysis of variance and adequacy of the quadratic model.

Source	Sum of squares	Degree of freedom	Mean square	F-value	P-value Prob >F	
Model	8371.5	14	597.96	42.77	< 0.0001	significant
A-pH	3847.12	1	3847.12	275.19	< 0.0001	
B-Time	495.41	1	495.41	35.44	< 0.0001	
C-Mass of catalyst	255.98	1	255.98	18.31	0.0007	
D-Concentration	610.65	1	610.65	43.68	< 0.0001	
AB	73.10	1	73.94	5.23	0.0372	
AC	250.43	1	583.95	17.91	0.0007	
AD	630.01	1	14.18	0.34	< 0.0001	
BC	22.94	1	748.84	17.88	0.2196	
BD	271.76	1	236.70	5.65	0.0005	
CD	7.13	1	387.30	9.25	0.4861	
A2	0.98	1	1701.36	40.63	0.7946	
B2	777.27	1	1789.97	42.74	< 0.0001	
C2	518.92	1	345.10	8.24	< 0.0001	
D2	209.70	1	727.36	17.37	< 0.0001	
Residual	200.64	15	41.88			
Lack of Fit	9.06	10	59.76	9.76		
Pure Error	8581.20	5	6.12		0.0801	significant
		29				

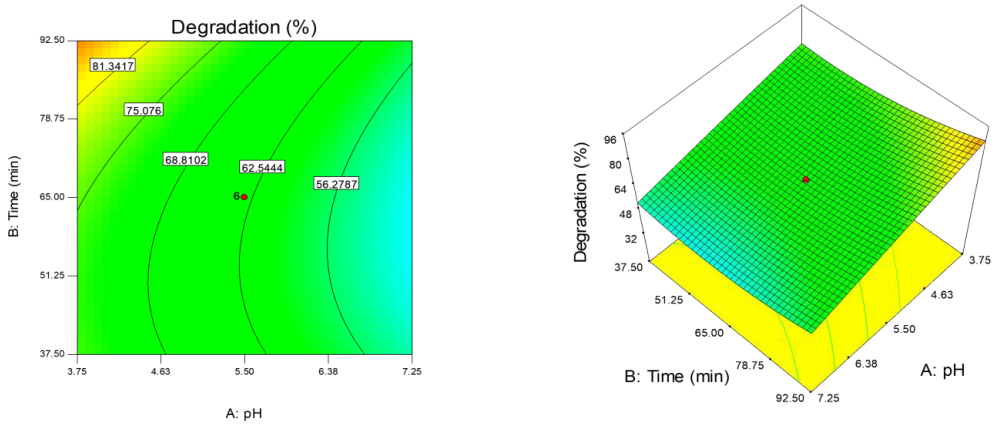

(a) (b)

Fig. 11. The effect of pH and time for degradation erythromycin a) Contour and b) 3D plot.

effective parameters in photocatalytic reactions. In order to determine the optimal pH, solutions with different pHs were prepared. The results indicate that the oxidation and degradation percentages of erythromycin are affected by the pH of the environment. Based on the results concluded that with decreasing pH, the efficiency of photocatalytic degradation increases because at low pH, direct reduction by electrons in the conduction band plays an important role in the decomposition of erythromycin degradation, which leads to a reduction gap in degradation of erythromycin. Also, the pKa of erythromycin is 8.9. Degradation time is one of the most important parameters in erythromycin degradation. High degradation time causes higher energy consumption and refining costs. Therefore, optimizing the process time saves operating costs. In this study the results showed that with increasing reaction time, the efficiency should increase. Fig. 11 shows the effect of pH and

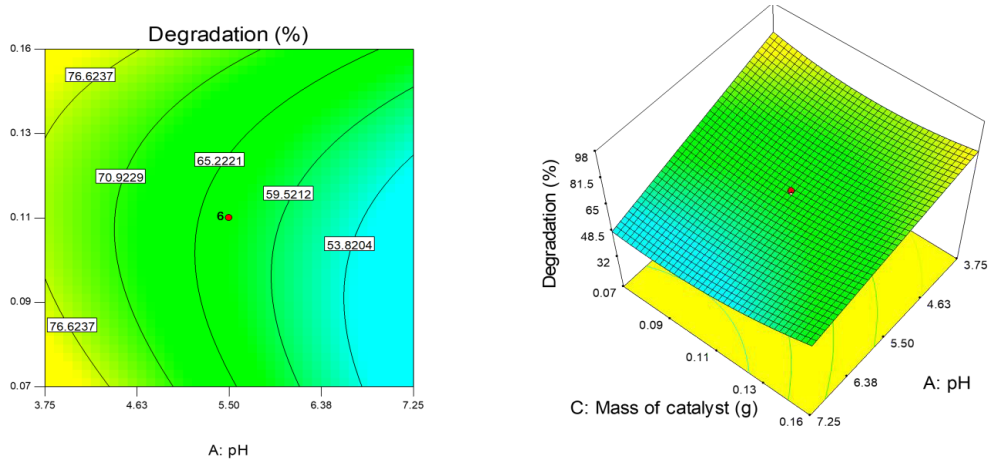

Fig. 12. The effect of pH and mass of catalyst for degradation of erythromycin a) Contour and b) 3D plot.

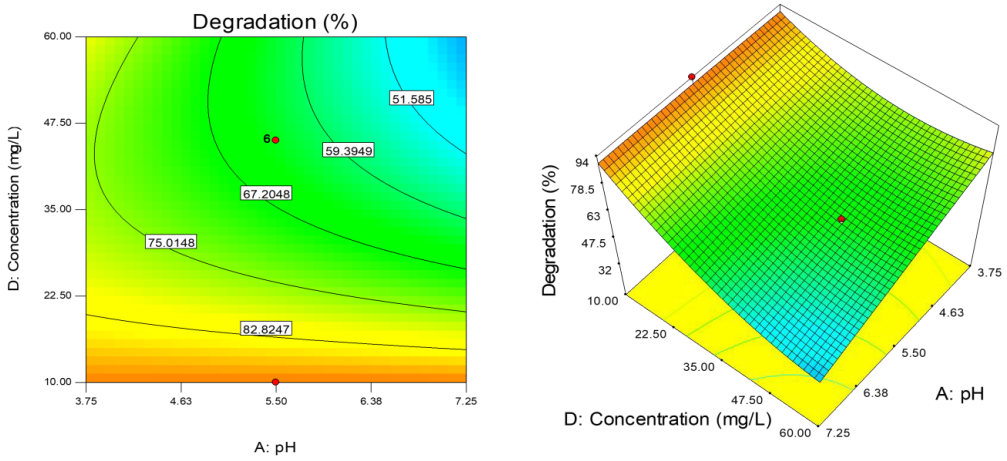

(a) (b)

Fig. 13. The effect of pH and mass of concentration of erythromycin for degradation of erythromycin a) Contour and b) 3D plot.

time on erythromycin degradation efficiency as contour and 3D plots.

Effect of pH and photocatalyst mass on erythromycin degradation efficiency

Catalyst mass is one of the important factors in the degradation process. As the amount of catalyst increases, the efficiency also increases, but this increase has some good performance and more than this amount will have the opposite effect on the amount of efficiency. The reason for this is that by increasing the amount of catalyst, the number of active sites is increased, which increases the efficiency of degradation. On the other hand, increasing the amount of catalyst reduces the penetration of light into the solution due to the increased turbidity of the solution because of the presence of catalyst particles on erythromycin degradation efficiency as contour and 3D plots (Fig.12).

Effect of pH and erythromycin concentration on erythromycin degradation efficiency

To investigate the effect of erythromycin concentration, experiments in the range of 10-60 mg/L were performed. The decrease in efficiency versus the increase in concentration can be explained by the fact that with increasing

Table 7. Isotherms and error functions for p-NiO/n-ZnO flower-like (5%).

Isotherm	isotherm parameter	Error & R^2	Error Value & R^2
Langmuir		HYBRID	77.189
q_m	123.21	MPSD	2.025
b_L	0.13	ARE	0.8853
		R^2	0.6542
Freundlich		HYBRID	3.218
K_f	2.7074E-08	MPSD	0.1357
N	0.3196	ARE	0.1696
		R^2	0.9740
Tempkin		HYBRID	11.773
B_T	0.0015	MPSD	0.1525
A_T	230.12	ARE	0.3328
		R^2	0.8872
Redlich-Peterson		HYBRID	27.0418
K_R	0.1995	MPSD	0.6173
a_R	3.6869	ARE	0.5856
G	0.2312	R^2	0.8086
Khan			
q_s	0.00005	HYBRID	4.1436
b_{KH}	0.530	MPSD	0.0862
a_{KH}	2.4958	ARE	0.2251
		R^2	0.9766
Radke-Prausnitz		HYBRID	4.1806
a_{RP}	6.098	MPSD	0.0485
r_{RP}	2740	ARE	0.1478
B_{RP}	1.710	R^2	0.9622
Fritz-Schlunder (IV)		HYBRID	1.4687
C	5.3194	MPSD	0.0017
D	3.4203	ARE	0.0045
α_{FS}	0.0001	R^2	0.9963
β_{FS}	0.097		

concentration of pollutants, the emitted radiation is absorbed by the pollutant molecules and does not reach the surface of photocatalysts. Fig. 13 shows the effect of examining the effect of pH and erythromycin concentration on erythromycin degradation efficiency as contour and 3D plots.

Optimization

Finally, the software determination at the best point to achieve the highest degradation efficiency of erythromycin, in optimal conditions is with p-NiO/n-ZnO (5%) mass of photocatalyst 0.13 (g), time 101.14 (min), erythromycin concentration 41.04 (mg/L) and pH= 3.07 99.99% (Fig. 14) [38, 39].

Isothermal study

Experimental data were studied with 2, 3 and 4 parametric isotherms and finally minimized by 3 error models (HYBRID, MPSD and ARE). The results of isothermal studies demonstrate that the Fritz-Schlunder isotherm has the best fit with the least error with the experimental data of p-NiO/n-ZnO photocatalytic degradation (Table 7) [40].

CONCLUSION

In this study, ZnO and NiO were loaded on a ZnO flower like. Degradation of erythromycin antibiotic was examined by the photocatalysts synthesized under sunlight. Flower like p-NiO/n-ZnO (5%) had the highest degradation efficiency

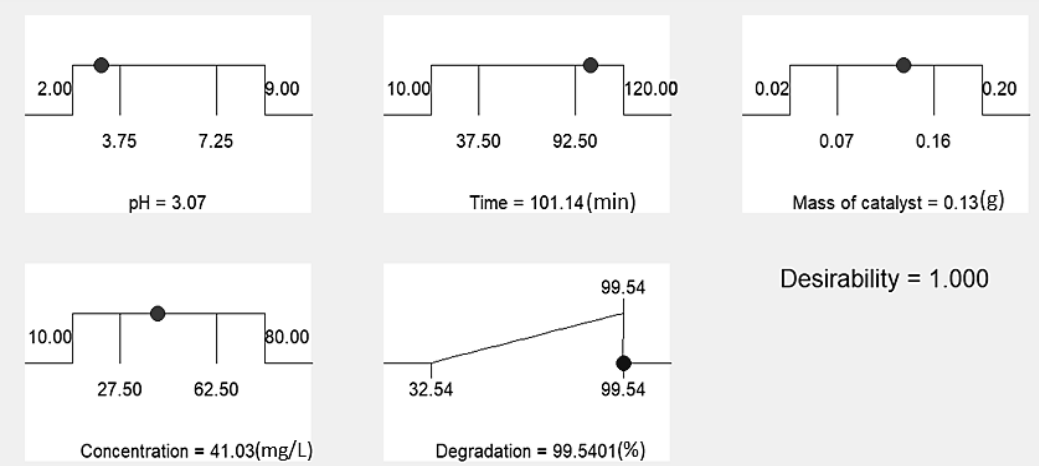

Fig. 14. Graphs of the optimum condition for degradation of erythromycin.

of erythromycin among the photocatalysts. Degradation of erythromycin by p-NiO/n-ZnO (5%) was investigated using RSM and according to the actual and predicted values of the software, the results showed that the statistical analysis of the software was highly accurate and also the effect of various parameters was well expressed and analyzed. Optimal conditions of photocatalytic degradation of erythromycin at pH 3.07, time 101.14 (min), photocatalytic mass 0.13 (g) and erythromycin concentration 41.04 (mg/L) were obtained 99.99%. Isothermal studies have shown that the Fritz-Schlander isotherm with the least error with the experimental data of p-NiO/n-ZnO (5%) photocatalytic degradation are the best fit.

CONFLICT OF INTEREST

The authors declare no conflicts of interest.

REFERENCES

[1]. N Kulik, M Trapido, A Goi, Y Veressinina, & R Munter. Chemosphere, 70 (8) 1525-1531 (2008). https://doi.org/10.1016/j.chemosphere.2007.08.026. https://doi.org/10.1016/j.chemosphere.2007.08.026

[2]. M Darzipour, M Jahanshahi, M Peyravi, M, & S Khalili, S. J. Chem. Eng, 36(12), 2035-2046 (2019). https://doi.org/10.1007/s11814-019-0391-y. https://doi.org/10.1007/s11814-019-0391-y

[3]. S.S. Fekr, N.E. Fard, & R Fazaeli, Russ. J. Appl. Chem, 94(6), 824-834 (2021). https://doi.org/10.1134/S1070427221060161. https://doi.org/10.1134/S1070427221060161

[4]. T.H Le, C Ng, N.H. Tran, H Chen, & K.Y.H. Gin. Water. Res, 145, 498-508 (2018). https://doi.org/10.1016/j.watres.2018.08.060. https://doi.org/10.1016/j.watres.2018.08.060

[5]. K Slipko, D Reif, M Woegerbauer, P Hufnagl, J Krampe, & N Kreuzinger. Water. Res, 164, 114916 (2019). https://doi.org/10.1016/j.watres.2019.114916. https://doi.org/10.1016/j.watres.2019.114916

[6]. S Ren, X Guo, A Lu, X Guo, Y Wang, G Sun, & L Wang. Bioresour. Technol, 265,155-162 (2018). https://doi.org/10.1016/j.biortech.2018.05.087. https://doi.org/10.1016/j.biortech.2018.05.087

[7]. A Payan, A. A Isari, & N Gholizade. Chem. Eng. J, 361, 1121-1141 (2019). https://doi.org/10.1016/j.cej.2018.12.118. https://doi.org/10.1016/j.cej.2018.12.118

[8]. T .K. Kim, T. Kim, Y Cha, & K.D Zoh, Water. Res, 185, 116159 (2020). https://doi.org/10.1016/j.watres.2020.116159. https://doi.org/10.1016/j.watres.2020.116159

[9]. Y Zhang, H Liu, Y Xin, Y Shen, J Wang, C Cai, & M Wang. Chem. Eng. J, 358, 1446-1453 (2019). https://doi.org/10.1016/j.cej.2018.10.157. https://doi.org/10.1016/j.cej.2018.10.157

[10]. L Chu, R Zhuan, D Chen, J Wang, & Y Shen, Chem. Eng. J, 361,156-166 (2019).. https://doi.org/10.1016/j.cej.2018.12.072. https://doi.org/10.1016/j.cej.2018.12.072

[11]. S Gaurav, K Amit, M Naushad, A García-Peñas, A.H Al-Muhtaseb, A.A Ghfar, & F Stadler. J. Carbohydrate Polymers, 202, 444-453 (2018). https://doi.org/10.1016/j.carbpol.2018.09.004. https://doi.org/10.1016/j.carbpol.2018.09.004

[12]. G Sharma, A Kumar, K Devi, S Sharma, M Naushad, A.A Ghfar, & F Stadler. J. Int. J. Biol. Macromol. 114, 295-305 (2018). https://doi.org/10.1016/j.ijbiomac.2018.03.093. https://doi.org/10.1016/j.ijbiomac.2018.03.093

[13]. G Sharma, D.D Dionysiou, S Sharma, A Kumar, H Ala'a, M Naushad, & F. J. Stadler, Catal. Today, 335, 437-451 (2019). https://doi.org/10.1016/j.cattod.2019.03.063. https://doi.org/10.1016/j.cattod.2019.03.063

[14]. P.A Sheena, K.P Priyanka, A Sreedevi, & T Varghese. J Nanostructure Chem, 8(2), 207-215 (2018). https://doi.org/10.1007/s40097-018-0272-7. https://doi.org/10.1007/s40097-018-0272-7

[15]. G Boczkaj, & A Fernandes. Chem. Eng. J. 320, 374-384 (2017). https://doi.org/10.1016/j.jclepro.2018.05.207.

https://doi.org/10.1016/j.jclepro.2018.05.207
[16]. N. E. Fard, R. Fazaeli, M. Yousefi, Sh. Abdolmohammadi, Chem. Select., 4(33), 9529-9539 (2019).https://doi.org/10.1002/slct.201901514. https://doi.org/10.1002/slct.201901514
[17]. N. E. Fard, R. Fazaeli, M. Yousefi, Sh. Abdolmohammadi, Appl. Physic. A., 125(9), 632-646 (2019). https://doi.org/10.1007/s00339-019-2918-9. https://doi.org/10.1007/s00339-019-2918-9
[18]. N. E. Fard, R. Fazaeli, Russ. J. Physic. Chem. A., 92(13), 2835-2846 (2018). https://doi.org/10.1007/s11814-015-0053-7. https://doi.org/10.1007/s11814-015-0053-7
[19]. N. E. Fard, R. Fazaeli, Int. J. Chem. Kinet., 48(11), 691-701 (2016). https://doi.org/10.1007/s11814-015-0053-7. https://doi.org/10.1007/s11814-015-0053-7
[20]. N. E. Fard, R. Fazaeli, Iran. J. Catal., 8(2), 133-141 (2018). https://doi.org/10.1002/kin.21025. https://doi.org/10.1002/kin.21025
[21]. L Zhu, Y Li, & W Zeng. Appl. Surf. Sci, 427, 281. 281-287 (2018). https://doi.org/10.1016/j.apsusc.2017.08.229. https://doi.org/10.1016/j.apsusc.2017.08.229
[22]. W Li, H Xu, H Yu, T Zhai, Q Xu, X Yang, & B Cao. J. Alloys Compd, 706, 461. 131-140 (2017). https://doi.org/10.1016/j.apcata.2015.02.013. https://doi.org/10.1016/j.apcata.2015.02.013
[23]. A.B Djurišić, X Chen, Y.H Leung, & A.M.C Ng. J. Mater. Chem, 22(14), 6526-6535 (2012). https://doi.org/10.1039/C2JM15548F. https://doi.org/10.1039/c2jm15548f
[24]. Y Zheng, B Zhu, H Chen, W You. C Jiang, & J.J Yu. Colloid Interface Sci, 504, 688-696 (2017). https://doi.org/10.1016/j.jcis.2017.06.014. https://doi.org/10.1016/j.jcis.2017.06.014
[25]. R.S Kate, S.A. Khalate, & R. J. J. Deokate, Alloys. Compd, 734, 89. 89-111 (2018). https://doi.org/10.1016/j.jallcom.2017.10.262. https://doi.org/10.1016/j.jallcom.2017.10.262
[26]. A Roychoudhury, S Basu, & S.K. Jha. Biosens. Bioelectron, 84, 72-81 (2016). https://doi.org/10.1016/j.bios.2015.11.061. https://doi.org/10.1016/j.bios.2015.11.061
[27]. W Nie, H Tsai, J.C Blancon, F Liu, C.C Stoumpos, B Traore,... & Crochet. J. Adv. Mater, 30(5), 1703879 (2018) https://doi.org/10.1002/adma.201703879. https://doi.org/10.1002/adma.201703879
[28]. J M Choi, J.H Byun, & S.S Kim, Sens. Actuators B Chem, 227, 149-156 (2016). https://doi.org/10.1016/j.snb.2015.12.014. https://doi.org/10.1016/j.snb.2015.12.014
[29]. A Meng, & J Yu, 31, 161-191 (2020). https://doi.org/10.1016/B978-0-08-102890-2.00005-1. https://doi.org/10.1016/B978-0-08-102890-2.00005-1
[30]. A. K Rana, M Kumar, D.K Ban, C.P Wong, J Yi, & J Kim. Adv. Electron. Mater, 5(8), 1900438 (2019). https://doi.org/10.1002/aelm.201900438. https://doi.org/10.1002/aelm.201900438
[31]. R. Fazaeli, & N.E. Fard, Russ. J. Appl. Chem. 93(7), 973-982 (2020). https://doi.org/10.1134/S1070427220070058. https://doi.org/10.1134/S1070427220070058
[32]. N. Kashi, N.E. Fard, R. Fazaeli. Russ. J. Appl. Chem. 90, 977 (2017). https://doi.org/10.1134/S1070427217060210. https://doi.org/10.1134/S1070427217060210
[33]. G. Li, B. Wang, J Zhang, R Wang, & H Liu, Appl. Surf. Sci. 478, 1056. 1056-1064 (2019). https://doi.org/10.1016/j.apsusc.2019.02.035. https://doi.org/10.1016/j.apsusc.2019.02.035
[34]. L Fernández, M Gamallo, M.A González-Gómez, C Vázquez-Vázquez, J Rivas, M Pintado, & M T Moreira, J. Environ. Manage, 237, 595-608 (2019). https://doi.org/10.1016/j.jenvman.2019.02.089. https://doi.org/10.1016/j.jenvman.2019.02.089
[35]. A Jana, N.R Bandyopadhyay, & P.S. Devi. Solid State Sciences, 13(8), 1633-1637 (2011). https://doi.org/10.1016/j.solidstatesciences.2011.06.015. https://doi.org/10.1016/j.solidstatesciences.2011.06.015
[36]. S Khamani, M.H Ghorbani, L Torkian, R Fazaeli, & Z Khodadadi, Russ. J. Phys. Chem. A, 95(10), 2154-2162 (2021). https://doi.org/10.1134/S0036024421100113. https://doi.org/10.1134/S0036024421100113
[37]. R Saadi, Z Saadi, R Fazaeli, & N.E Fard. J. Chem. Eng, 32(5), 787-799(2015).https://doi.org/10.1007/s11814-015-0053-7. https://doi.org/10.1007/s11814-015-0053-7
[38]. S. A. K, Vandani, R. Fazaeli, M. G. Saravani, & H. Pasdar, Egypt. J. Chem, 64(10), 3-4 (2021). 0.21608/ejchem.2021.33523.2703.
[39]. S. A. K, Vandani, R. Fazaeli, M. G. Saravani, & H. Pasdar, J. Environ. Eng. Sci, 40(XXXX), 1-11 (2021). https://doi.org/10.1680/jenes.20.00018. https://doi.org/10.1680/jenes.20.00018
[40]. N. E. Fard, R. Fazaeli, & R. Ghiasi. Chem. Eng. Technol, 39(1), 149-157 (2016). https://doi.org/10.1002/ceat.201500116. https://doi.org/10.1002/ceat.201500116